

A Numerical Study on Helix Nanowire Metamaterials as Optical Circular Polarizers in the Visible Region

Z. Y. Yang, M. Zhao, and P. X. Lu

Abstract—Broadband optical circular polarizers functioning in the visible region were developed based on structural design and numerical simulation using the finite-difference time-domain method. By properly selecting the parameters of helix nanowire metamaterials including metal materials, diameters of wires, numbers of helix-period, spacing of grids, lengths of helix-period, and diameters of helices, we proposed a broadband optical circular polarizer using aluminium helix nanowire metamaterials on a silica substrate. The proposed polarizer can reach an extinction ratio above 39:1 and a transmission efficiency above 64% in the range from 410 to 790 nm.

Index Terms—Optical polarization, superlattices.

I. INTRODUCTION

OPTICAL circular polarizations of light are attractive for applications in reflective color displays [1], life science microscopies, and photography [2]. Generally, there are two ways of obtaining circular polarized light: one is using a linear polarizer and a quarter-wave plate [3], which is the most common method in optical applications; the other is utilizing cholesteric liquid crystals (CLCs) [4], which are self-assembled photonic crystals formed by rodlike molecules. However, all these methods have been restricted to narrow frequency ranges, which is a major drawback for many potential applications [5].

Recently, it was reported that Gansel [5], [6] succeeded in developing a broadband circular polarizer by using gold helix metamaterials. The device had high performance in the region of 3–6 μm . In such a helical structure, the circularly polarized light with the opposite handedness to the helix propagating along the helical axis is selectively transmitted. Compared with the former two methods, the helical circular polarizer has advantages of broad frequency ranges, and compact structures which are convenient to integrating with other optical devices. However, references [5] and [6] were focused on the range of infrared, and did not analyze the influences of the parameters in the visible region. Therefore, it is now very timely to develop a device structure which can operate in the broad visible range, and study the

Manuscript received March 12, 2010; revised April 29, 2010; accepted June 19, 2010. Date of publication June 28, 2010; date of current version August 11, 2010. This work was supported by the Natural Science Foundation of China (NSFC) (10874024 and 50735007), by the Doctoral Fund of Ministry of Education of China (200804871147), by the Natural Science Foundation of Hubei Province of China (2008CDB004), and in part by China National Funds for Distinguished Young Scientists (66945021), and the “973” Program of China (2010CB923203).

The authors are with Wuhan National Laboratory for Optoelectronics, Huazhong University of Science and Technology, Wuhan, Hubei 430074, China (e-mail: zyang@mail.hust.edu.cn; lupeixiang@mail.hust.edu.cn).

Color versions of one or more of the figures in this letter are available online at <http://ieeexplore.ieee.org>.

Digital Object Identifier 10.1109/LPT.2010.2054073

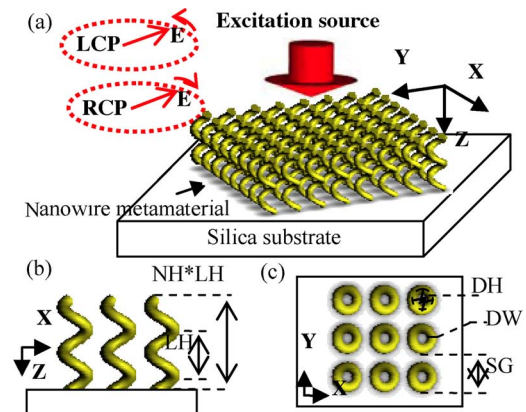


Fig. 1. Schematic diagram of the circular polarizer used in simulations.

influences of the parameters. Although there were some theoretical studies on helical structures [7]–[10], most of them were focused on dielectric materials but not on metallic materials. In this letter, the finite-difference time-domain (FDTD) method was used to design broadband optical circular polarizers with helix nanowire metamaterials, which can operate in the visible region. By analyzing the parameters of the helix nanowire metamaterials including metal materials, diameters of wires (DW), numbers of helix-period (NH), spacing of grids (SG), lengths of helix-period (LH), and diameters of helices (DH), we proposed a broadband optical circular polarizer using aluminium helix nanowire metamaterials on a silica substrate.

II. SIMULATION MODELS

Helix nanowire metamaterials were used as the basic structure to design polarizers. Six parameters, metal materials, diameters of wires, numbers of helix-period, spacing of grids, lengths of helix-period, and diameters of helices, are critical to determine the optical performance of the broadband optical circular polarizer. Fig. 1 shows the schematic diagram of the device structure used in the simulation. Helix nanowire layers were placed on a silica substrate with refractive index of 1.5. The medium around the nanowire is air. Two circularly polarized states of light, left-handed circular polarization (LCP) and right-handed circular polarization (RCP), were used as excitation sources. The source illuminated the nanowire metamaterial along the positive Z -direction for LCP and RCP light, respectively. In the calculations, the excitation source is a broadband Gaussian-modulated pulsed light source. The perfectly matched layers (PMLs) [11] were along the Z -direction. The boundaries along the X - and Y -directions were confined with the periodic boundary conditions (PBCs) [12] due to the periodicity of the

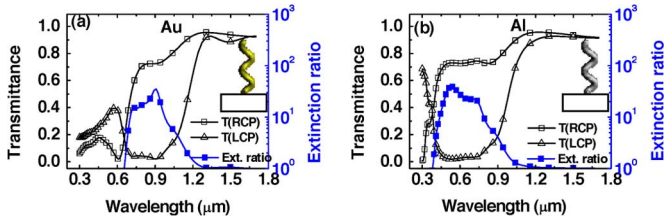


Fig. 2. Transmittances of RCP, LCP light and extinction ratios of polarizers with different metal materials: (a) Au and (b) Al.

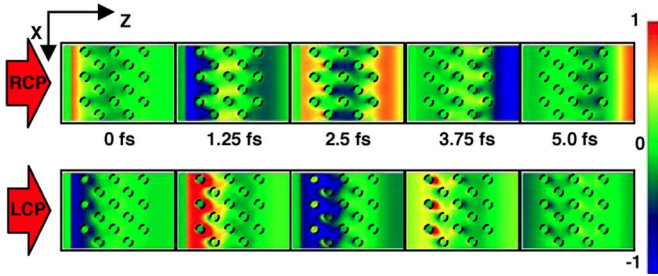


Fig. 3. Propagation of the RCP and LCP light through the Al helix nanowire circular polarizer.

nanowire metamaterial. This simplification of periodic condition greatly reduced the computation time.

III. SIMULATION RESULTS AND ANALYSES

Helix nanowire grids with different metal materials, gold (Au), silver (Ag), chromium (Cr), and aluminium (Al), were simulated. The parameters of the nanowire grids are: DW = 50 nm, NH = 2, SG = 190 nm, LH = 200 nm, and DH = 100 nm. During the calculation, the dielectric functions of the metal materials were described by the Lorentz–Drude model [13]. The optical performances of the Au and Al helix nanowire polarizers are shown in Figs. 2(a) and (b), respectively. In these figures, the transmittance of the LCP (RCP) light is the ratio of the LCP (RCP) transmitted light intensity and the LCP (RCP) incident light intensity. The extinction ratio refers to the ratio of the transmittance of the RCP light and the transmittance of the LCP light. From the simulation results, the functional wavelength regions, the average transmittances of the RCP light and the average extinction ratios of the polarizers with Ag, Au, Cr, and Al helix nanowire grids are obtained as follows: (0.63–0.92 μm , 73%, 19 : 1), (0.72–0.96 μm , 69%, 19 : 1), (0.45–0.75 μm , 41%, 8 : 1), and (0.46–0.77 μm , 73%, 27 : 1). Fig. 3 shows the processes of the RCP and LCP light propagating through the Al circular polarizer. It is clear that most of the RCP light is transmitted through the Al helix nanowire, but the LCP light is not. From the simulation results, it becomes obvious that the Al helix nanowire circular polarizers have the best optical performance in the range of the visible wavelength. The reason is that Al has a larger plasma frequency than those of Ag, Au, and Cr, which leads to relatively large real and imaginary parts of the optical dielectric function of Al [13]. Therefore, while the circularly polarized light with the same handedness to the helix propagates along the helical axis, the Al nanowire has a higher reflectance than

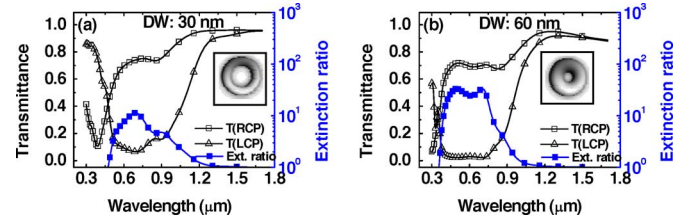


Fig. 4. Transmittances of RCP, LCP light and extinction ratios for different DW.

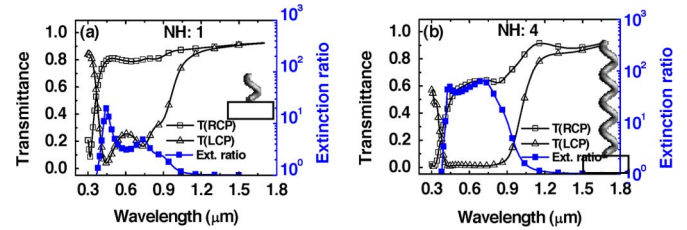


Fig. 5. Transmittances of RCP, LCP light and extinction ratios for different NH.

the other metal wires. Thus, Al was selected as the metallic material for the broadband circular polarizer.

Structures of Al helix nanowire-grid circular polarizers with different DW were calculated. The other parameters are fixed to their respective values in Fig. 2(b). When the DW is 30, 40, 50, and 60 nm, the functional wavelength regions, the average transmittances of the RCP light, and the average extinction ratios are (0.53–0.94 μm , 75%, 6.3 : 1), (0.5–0.75 μm , 73%, 19.7 : 1), (0.46–0.77 μm , 73%, 27 : 1), and (0.4–0.77 μm , 69%, 26.3 : 1), respectively. The transmittance of the RCP, LCP light and the extinction ratio for DW of 30 and 60 nm are shown in Fig. 4. Structures with different SG were also simulated. When the SG is 390, 290, and 190 nm, the functional wavelength regions, the average transmittances of the RCP light and the average extinction ratios are (0.52–0.76 μm , 90%, 3.3 : 1), (0.55–0.73 μm , 85%, 8.8 : 1), and (0.46–0.77 μm , 73%, 27 : 1), respectively. Al helix nanowire circular polarizers with different NH were also simulated. When NH is 1, 2, 3, and 4, the functional wavelength regions, the average transmittances of the RCP light and the average extinction ratios are (0.42–0.49 μm , 79%, 6.3 : 1), (0.46–0.77 μm , 73%, 27 : 1), (0.42–0.79 μm , 64%, 39.7 : 1), and (0.42–0.83 μm , 58%, 46.3 : 1), respectively. The optical performances of the polarizers with different NH are shown in Fig. 5. From the calculation results, it is clear that the larger DW or smaller SG or more NH leads to higher extinction ratios, which can be explained that increasing the DW or decreasing the SG or enlarging the NH gives rise to stronger scattering from the nanowire. However, the circular polarizer with large DW, small SG and more NH also has a lower transmittance of RCP light. Therefore, the DW with 50–60 nm, the SG with 190 nm, and three helix-periods are chosen for the broadband circular polarizer in the visible region.

We also simulated structures with different LH. The other parameters are fixed to their respective values in Fig. 2(b). When LH is 150, 200, 300, and 400 nm, the functional wavelength regions, the average transmittances of the RCP light, and the average extinction ratios are (0.39–0.79 μm , 67%, 12.1 : 1),

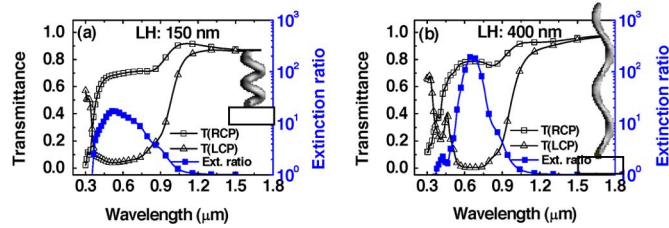


Fig. 6. Transmittances of RCP, LCP light and extinction ratios for different LH.

(0.46–0.77 μm , 73%, 27 : 1), (0.50–0.75 μm , 77%, 72 : 1), and (0.58–0.75 μm , 78%, 138 : 1), respectively. The optical performances of the polarizers with LH = 150 and 400 nm are shown in Fig. 6. From the simulation results, it becomes obvious that the extinction ratio is enhanced with the increase of the LH. However, the increase of the LH also leads to the narrowing of the functional region. The functional region of the metal helix is determined by the interplay of pronounced internal resonances and their mutual coupling, which gives rise to the broadband response [5]. When the LH is increased, the interaction among the periodical unit cell is weakened. For this reason, the functional wavelength region is narrowed with the increase of the length of helix-period. Based on the simulation results, an LH around 200 nm is an ideal value for the broadband circular polarizer.

Finally, Al helix structures with different DH were simulated. The values of other parameters are the same with those in Fig. 2(b) except of SG. When DH is 100, 200, and 300 nm, SG is set with 190, 290, and 390 nm. The functional wavelength regions, the average transmittances of the RCP light, and the average extinction ratios are as follows: (0.46–0.77 μm , 73%, 27 : 1), (0.64–1.3 μm , 48%, 14 : 1), and (0.97–1.6 μm , 37%, 11 : 1). The optical performances of the polarizers with DH = 100 and 200 nm are shown in Fig. 7. From these simulation results, it is clear that with the increase of the DH, the functional region has a red shift. Following antenna theory, the strongest dependence of the resonance positions is expected when varying the DH. While the DH is increased, the resonance wavelength has a red shift, which leads to the red shift of the functional region [6].

IV. CONCLUSION

In summary, broadband helix nanowire circular polarizers for the visible region were designed using the FDTD method. The parameters, wire materials, DW, NH, SG, LH, and DH, can greatly affect the optical performance of the polarizer. According to the simulation results, the structure with Al nanowire, DW of 50 nm, NH of 3, SG of 190 nm, LH of 200 nm, and

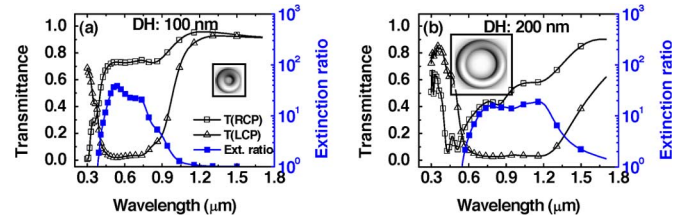


Fig. 7. Transmittances of RCP, LCP light and extinction ratios for different DH.

DH of 100 nm, can reach the optical performance of an extinction ratio above 39 : 1, a transmission efficiency above 64%, and functional wavelength range from 410 to 790 nm. Although, it is certain that there are still some challenges on the fabrication of the polarizer: how to etch such small three dimensional patterns, and deposit Al nanowire on the patterns uniformly. It is expected that with the development of nanofabrication techniques, the broadband circular polarizer will be realized.

REFERENCES

- [1] G. De Filpo, F. P. Nicoletta, and G. Chidichimo, "Cholesteric emulsions for colored displays," *Adv. Mater.*, vol. 17, pp. 1150–1152, 2005.
- [2] K. Claborn, E. Puklin-Faucher, M. Kurimoto, W. Kaminsky, and B. Kahr, "Circular dichroism imaging microscopy: Application to enantiomorphous twinning in biaxial crystals of 1,8-dihydroxyanthraquinone," *J. Amer. Chem. Soc.*, vol. 125, pp. 14825–14831, Dec. 2003.
- [3] E. Hecht, "Polarization," in *Optics*, 4th ed. San Francisco, CA: Addison-Wesley, 2002, pp. 357–358.
- [4] N. Y. Ha *et al.*, "Fabrication of a simultaneous red-green-blue reflector using single-pitched cholesteric liquid crystals," *Nat. Mater.*, vol. 7, pp. 43–47, Jan. 2008.
- [5] J. K. Gansel *et al.*, "Gold helix photonic metamaterial as broadband circular polarizer," *Science*, vol. 325, pp. 1513–1515, 2009.
- [6] J. K. Gansel, M. Wegener, S. Burger, and S. Linden, "Gold helix photonic metamaterials: A numerical parameter study," *Opt. Express*, vol. 18, pp. 1059–1069, Jan. 2010.
- [7] I. Abdulhalim, "Light-propagation along the helix of chiral smectics and twisted nematics," *Opt. Commun.*, vol. 64, pp. 443–448, 1987.
- [8] I. Abdulhalim, "Effect of the number of sublayers on axial optics of anisotropic helical structures," *Appl. Opt.*, vol. 47, pp. 3002–3008, 2008.
- [9] P. D. Sunal, A. Lakhtakia, and R. Messier, "Simple model for dielectric thin-film helicoidal bianisotropic media," *Opt. Commun.*, vol. 158, pp. 119–126, 1998.
- [10] J. C. W. Lee and C. T. Chan, "Polarization gaps in spiral photonic crystals," *Opt. Express*, vol. 13, pp. 8083–8088, 2005.
- [11] J. P. Berenger, "A perfectly matched layer for the absorption of electromagnetic-waves," *J. Comput. Phys.*, vol. 114, pp. 185–200, 1994.
- [12] P. Harms, R. Mittra, and W. Ko, "Implementation of the periodic boundary condition in the finite-difference time-domain algorithm for FSS structures," *IEEE Trans. Antennas Propagat.*, vol. 42, no. 9, pp. 1317–1324, Sep. 1994.
- [13] D. Rakic, A. B. Djuric, J. M. Elazar, and M. L. Majewski, "Optical properties of metallic films for vertical-cavity optoelectronic devices," *Appl. Opt.*, vol. 37, pp. 5271–5283, 1998.